

## Nuclear-magnetic-resonance study of the cubic alkali tungsten bronzes\*

B. R. Weinberger<sup>†</sup>

Laboratory of Atomic and Solid State Physics and Materials Science Center,  
Cornell University, Ithaca, New York 14853

(Received 25 July 1977)

NMR measurements of the cubic alkali tungsten bronzes  $\text{Na}_x\text{WO}_3$  ( $0.22 \leq x \leq 0.84$ ) and  $\text{Li}_x\text{WO}_3$  ( $0.27 \leq x \leq 0.49$ ) are presented. Knight shifts, relaxation times, and line shapes of  $^{183}\text{W}$  were studied over the temperature range 1.35–4.2 K.  $T_1$  and  $K$  of  $^7\text{Li}$  at 77 and 298 K were also measured. These results coupled with previous  $^{23}\text{Na}$  measurements are correlated to possible conduction-band models. The results for  $x > 0.40$  are consistent with a  $W5d(t_{2g})$  conduction band analogous to the  $\text{Re } 5d(t_{2g})$  band in  $\text{ReO}_3$  band-structure calculations. For  $x < 0.40$  the data suggest admixture of Na and W  $6s$  states in the  $\text{Na}_x\text{WO}_3$  conduction band. Regarding the metal-semiconductor transition occurring in the bronzes, the NMR results seem incompatible with simple nearest-neighbor linkage and correlated site percolation models of conduction for the bronzes. The results give no evidence of a Mott-type transition occurring as no correlation effects are observable.

### INTRODUCTION

The alkali tungsten bronzes form a family of nonstoichiometric compounds with the formula  $M_x\text{WO}_3$ , where  $M$  represents the alkali atom and  $0 < x < 1$ . The bronzes exist in a variety of crystal symmetries depending upon the nature and concentration of the alkali atom.<sup>1</sup> The sodium and lithium bronzes have appreciable alkali concentration ranges over which a simple cubic "perovskite" phase is stable. These are the materials examined in this work. The electronic structure of the cubic alkali bronzes was probed through a NMR study of the  $^{183}\text{W}$  resonance in  $\text{Na}_x\text{WO}_3$  ( $0.22 \leq x \leq 0.84$ ) and the  $^{183}\text{W}$  and  $^7\text{Li}$  resonances in  $\text{Li}_x\text{WO}_3$  ( $0.27 \leq x \leq 0.49$ ).

For  $x > 0.25$ , the bronzes are metallic with Hall constant measurements<sup>2,3</sup> indicating that each alkali atom contributes one conduction electron. Near  $x = 0.25$  a transition from metallic to semiconducting behaviour occurs as a function of alkali concentration as indicated by a thermally activated component to the electrical conductivity and number of Hall carriers.<sup>2,4</sup> The NMR results obtained in this work provide interesting insights into the nature of this transition.

Detailed band-structure calculations are presently unavailable for the bronzes. Mattheiss, however, has carried out semiempirical band-structure calculations for several related materials, the perovskites  $\text{SrTiO}_3$ ,  $\text{KMoO}_3$ ,  $\text{KTaO}_3$ , and  $\text{ReO}_3$ .<sup>5,6</sup>  $\text{KMoO}_3$  and  $\text{ReO}_3$  have the same number of valence electrons as  $\text{NaWO}_3$  and like  $\text{NaWO}_3$  are metallic. The band structure of the perovskites studied by Mattheiss evidence remarkable similarities. A common feature is a broad  $d(t_{2g})$  conduction band broadened by  $\pi$  overlap with oxygen  $2p$  states. It has been observed that the density of

states versus energy histogram for the  $5d(t_{2g})$  conduction band of  $\text{ReO}_3$  is fit well by an exponential.<sup>7,8</sup>

$$\rho(E) = A \exp\left(\frac{E}{E_0}\right). \quad (1)$$

Equation (1) may be applied to  $\text{Na}_x\text{WO}_3$ .

$$\frac{x}{a^3} = \int_0^{E_F} \rho(E) dE, \quad (2)$$

where  $x/a^3$  is the number of conduction electrons per unit volume, if  $a$  is the lattice constant. This results in

$$\begin{aligned} x/a^3 &= E_0 A \exp(E_F/E_0) - E_0 A \\ &= E_0 [\rho(E_F) - A], \end{aligned} \quad (3)$$

$$\rho(E_F) = (E_0 a^3)^{-1} x + A.$$

This linearly varying density of states at the Fermi surface with  $x$ , the alkali concentration, has been observed in conduction-electron specific-heat<sup>9,9</sup> and magnetic-susceptibility<sup>8,10,11</sup> measurements performed on  $\text{Na}_x\text{WO}_3$  ( $0.22 \leq x \leq 0.90$ ). Observation of the concentration dependent Kohn effect<sup>12</sup> in sodium bronze crystals ( $0.56 \leq x \leq 0.83$ ) also agree with this rigid-band picture of the bronzes.

Nuclear magnetic resonance has proven to be a useful probe of the nature of conduction electron systems through the hyperfine interaction of the conduction electrons with the nuclei. The electrons by virtue of their spin and orbital magnetic moments produce magnetic fields at the nuclei, the average value of which produces a shift in the resonant magnetic field, the Knight shift

$$K = \Delta H/H_0 = (1/\beta) H_{\text{hf}} \chi. \quad (4)$$

The fluctuations of the hyperfine field  $H_{\text{hf}}$  result

in the nuclear-spin-lattice relaxation rate

$$(T_1)^{-1} = 4\pi\hbar(\gamma_n H_{\text{nr}})^2 \rho^2(E_F) kT\delta, \quad (5)$$

where  $\gamma_n$  is the nuclear gyromagnetic ratio,  $\beta$  is the Bohr magneton, and  $\delta$  is a numerical constant depending upon the electron-nuclear coupling mechanism.

Several previous NMR studies of the cubic sodium bronzes have been performed. The Knight shift<sup>13</sup> and spin-lattice relaxation rate<sup>14</sup> of  $^{23}\text{Na}$  in  $\text{Na}_x\text{WO}_3$  as well as the  $^{183}\text{W}$   $K$  (Ref. 15) and  $(T_1)^{-1}$  (Ref. 16) were measured in samples with  $x \approx 0.56$ . These results are consistent with a  $W 5d$  conduction-band model of the bronzes. Weaker coupling of the conduction electrons to the sodium nuclei than to the tungsten is indicated by  $^{23}\text{Na}$  Knight shifts and relaxation rates smaller by more than an order of magnitude than their  $^{183}\text{W}$  counterparts in the high- $x$  range. Furthermore, the  $^{183}\text{W}$  Knight shifts are negative, which is consistent with core polarization<sup>17</sup> by tungsten  $5d$  electrons being the dominant electron-tungsten-nucleus coupling mechanism.

Recent work by Tunstall<sup>7</sup> has extended the  $^{23}\text{Na}$  NMR measurements to the low-mobility concentration range ( $0.22 \leq x \leq 0.57$ ). He observed small- $x$ -independent negative Knight shifts ( $\approx -65$  ppm) consistent with previous results. The  $^{23}\text{Na}$  spin-lattice relaxation rate data is portrayed graphically in Fig. 1. Contrary to the earlier results of Fromhold and Narath,<sup>14</sup> the spin-lattice relaxation rates measured by Tunstall are strongly  $x$  dependent. The constancy of the earlier data with  $x$  has been attributed to sample impurities causing relaxation via paramagnetic impurities to be the dominant  $^{23}\text{Na}$  nuclear relaxation mechanism rather

than conduction electron relaxation.

The ordinate of Fig. 1 is  $(T_1 T)^{-1/2}$ . Assuming magnetic conduction electron relaxation to be dominant, according to Eq. (5), this quantity would be proportional to  $H_{\text{nr}}\rho(E_F)$ . Therefore, in a rigid-band model with sodium donating its outer electron to a  $W 5d(t_{2g})$  conduction band similar to the  $\text{Re } 5d(t_{2g})$  band in Mattheiss' calculations for  $\text{ReO}_3$ ,  $(T_1 T)^{-1/2}$  would vary linearly with  $x$ .

$$(T_1 T)^{-1/2} \propto (E_0 a^3)^{-1} x + A. \quad (6)$$

For  $x > 0.40$ , the data presented in Fig. 1 is not inconsistent with this prediction. However, the  $^{23}\text{Na}$  relaxation rates in the concentration range  $0.22 \leq x \leq 0.40$  evidence an enhancement not suggested by this rigid-band model of the cubic bronzes.

The results presented in this paper extend the  $^{183}\text{W}$  NMR measurements to the low mobility alkali concentration range ( $0.22 \leq x \leq 0.40$ ) and refine the results in the higher concentration range ( $0.57 \leq x \leq 0.84$ ) in  $\text{Na}_x\text{WO}_3$ . These results coupled with the  $^{23}\text{Na}$  data provide the basis for a plausible picture of the electronic structure of the metallic alkali tungsten bronzes in the concentration range approaching the metal-semiconductor transition.

#### EXPERIMENTAL DETAILS

Table I lists the alkali tungsten bronze samples used in this work. The low- $x$   $\text{Na}_x\text{WO}_3$  powders were prepared by Tunstall using crystals grown by Lilienfeld who also grew the  $\text{Li}_x\text{WO}_3$  crystals used in the preparation of the  $\text{Li}_x\text{WO}_3$  samples. Single crystals of high- $x$   $\text{Na}_x\text{WO}_3$  ( $\text{Li}_x\text{WO}_3$ ) were grown by electrolysis performed on a fused mixture of  $\text{Na}_2\text{WO}_4 \cdot 2\text{H}_2\text{O}$  ( $\text{Li}_2\text{WO}_4 \cdot 2\text{H}_2\text{O}$ ) and  $\text{WO}_3$ . Large cubic single crystals ( $1 \text{ cm}^3$  and larger) of  $\text{Na}_x\text{WO}_3$  with  $x \geq 0.57$  were produced. Smaller crystals of  $\text{Li}_x\text{WO}_3$  were produced in the range  $0.42 \leq x \leq 0.49$ . The lower  $x$  samples were produced by a dilution-diffusion technique described by Lightsey.<sup>18</sup> Samples were analyzed for verification of the cubic structure and determination of the lattice constant using a Debye-Scherrer powder x-ray camera. Both the lowest concentration  $\text{Na}_x\text{WO}_3$  and  $\text{Li}_x\text{WO}_3$  powders gave evidence of the imminent breakdown of the cubic structure as weak extra lines not arising from the simple cubic lattice were observed in the x-ray photograph. The lattice constant of the cubic sodium bronzes has been established as a reliable measure of the sodium content<sup>19,20</sup> and so was used as one determination of  $x$ . The variation of  $a$  with  $x$  is not accurately known for cubic  $\text{Li}_x\text{WO}_3$ , so only chemical analysis was relied

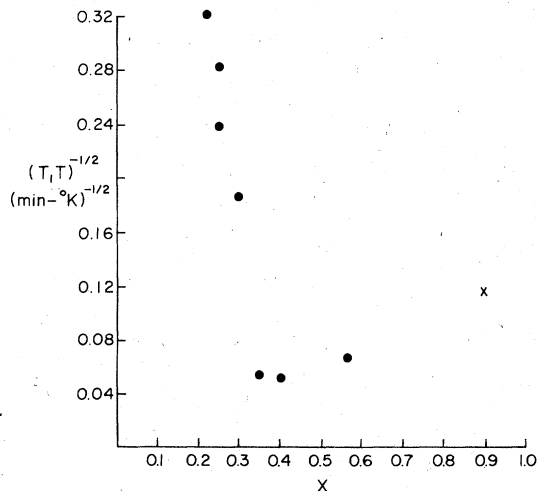


FIG. 1.  $^{23}\text{Na}$  spin-lattice relaxation rates at 4.2 K. —Data from Ref. 7. X—Data from Ref. 14.

upon for the determination of the lithium content. Samples were analyzed by the Chemical Analytical Laboratory of the Cornell University Materials Science Center. Results of atomic absorption spectroscopy determinations of alkali content are listed in Table I under chemical analysis. Impurity analysis by flame emission spectroscopy of crystalline material used in the diffusion runs showed calcium present at 100 ppm with no other impurities at levels greater than 10 ppm. In order to insure penetration of the rf magnetic field into the metallic bronze samples, all NMR experiments were performed on powdered samples. Crystalline samples were well ground and suspended in paraffin in order to insure electrical isolation of particles smaller in size than the 7-MHz skin depth.

The principle measurements in this study involved the observation of the NMR properties of the  $^{183}\text{W}$  nuclei in  $\text{Na}_x\text{WO}_3$  and  $\text{Li}_x\text{WO}_3$ .  $T_1$ , the spin-lattice relaxation time;  $K$ , the Knight shift; and  $\chi''(\omega)$ , the absorption line shape, were measured as a function of alkali concentration using pulse techniques over the temperature range 1.35–4.2 K. Also studied at 298 K and 77 K were  $T_1$  and  $K$  of  $^7\text{Li}$  in  $\text{Li}_x\text{WO}_3$ .

Tungsten has only one magnetic isotope,  $^{183}\text{W}$ , with a natural abundance of 14%. It has  $I = \frac{1}{2}$ , and hence a zero-electric-quadrupole moment, but has a very small magnetic moment which put stringent demands on the NMR spectrometer. A

pulsed NMR spectrometer was assembled based upon a Magnion superconducting solenoid and cryogenic system Model No. CF50-150-1000C which was operated at 40 kG. At that field, the  $^{183}\text{W}$  resonance occurred at 7 MHz. A single coil probe of two turns in the Helmholtz configuration delivering an  $H_1$  of 95 G over a sample volume of about  $1\text{ cm}^3$  was employed. Following phase coherent detection, the resulting signal-to-noise ratio for a  $^{183}\text{W}$  spin echo in  $\text{Na}_x\text{WO}_3$  at 4.2 K was approximately 2:1. Iterative signal averaging was then accomplished using a Biomation No. 610B transient recorder and a Nuclear Data No. ND 800 Enhancer memory unit.

$^7\text{Li}$  has a  $\gamma_n$  almost ten times as large as  $^{183}\text{W}$  and thus did not require the large  $H_0$  the  $^{183}\text{W}$  work did. The resonance was observed at 14 MHz, corresponding to a field of 8.5 kG obtained from a Harvey Wells electromagnet. Room-temperature  $K$  measurements of  $^7\text{Li}$  in  $\text{Li}_x\text{WO}_3$  were made with respect to an aqueous  $\text{Li}_2\text{SO}_4$  solution using cw techniques. The cw spectrometer was based upon a Varian V4230B crossed coil probe and V4210A variable frequency rf unit.

The measurements in this work were accomplished using standard pulsed NMR techniques. All  $^{183}\text{W}$  measurements were made on the spin echo which facilitated the separation of the nuclear signal from the ringdown of the transmitter pulse.  $T_1$  was measured by monitoring the recovery of the echo following a  $180^\circ$  pulse ( $180^\circ$ - $90^\circ$ - $180^\circ$  pulse

TABLE I. Samples used in this work.

Nominal $x$	Method of production	Chemical analysis $x$	X-ray $x$
$\text{Na}_x\text{WO}_3$			
0.22	Electrolysis and diffusion	0.22	0.18
0.25	Electrolysis and diffusion	0.26	0.25
0.30	Electrolysis and diffusion	0.31	0.30
0.35	Electrolysis and diffusion	0.36	0.37
0.40	Electrolysis and diffusion	0.40	0.42
0.57	Electrolysis	0.55	0.57
0.74	Electrolysis		0.74
0.84	Electrolysis		0.84
$\text{Li}_x\text{WO}_3$			X-ray $a$ (Å)
0.27	Electrolysis and diffusion	0.27	3.735
0.32	Electrolysis and diffusion	0.32	3.731
0.42	Electrolysis	0.42	3.722
0.49	Electrolysis	0.49	3.722

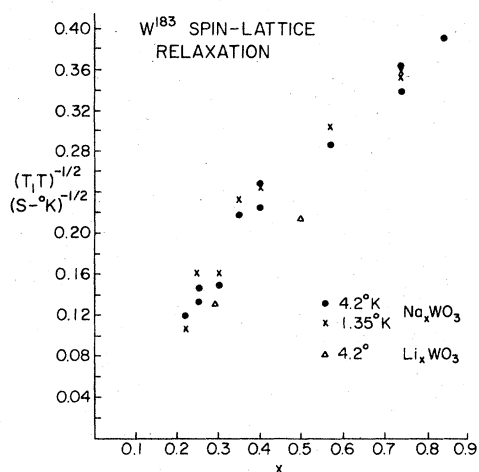


FIG. 2.  $^{183}\text{W}$  spin-lattice relaxation rates from this work.

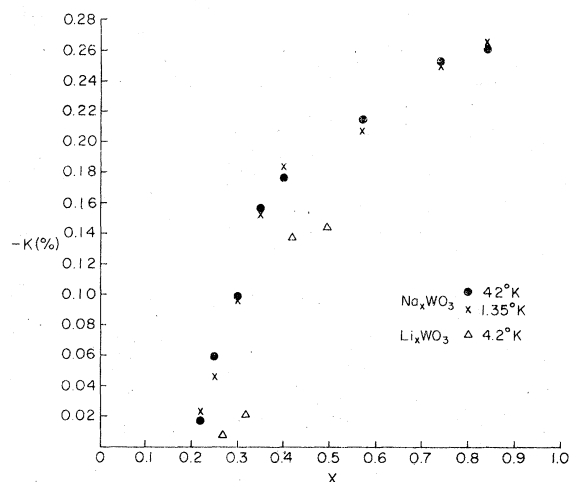


FIG. 3.  $^{183}\text{W}$  Knight-shift results from this work.

sequence). Knight shifts of  $^{183}\text{W}$  in the bronzes were determined by measuring the frequency shift of the center of gravity of the bronze resonance with respect to the  $^{183}\text{W}$  resonance in tungsten metal in a mixed bronze and metal sample at constant  $H_0$ . The center of each resonance was determined by studying the beat pattern in the echo as a function of frequency using phase coherent detection. The  $^{183}\text{W}$  line shapes in the sodium bronzes were obtained by integrating the full spin echo while sweeping the frequency, using a variation of the technique described by Clark.<sup>21</sup> The integration was performed using a PAR CW-1 boxcar integrator. The  $^7\text{Li}$   $T_1$ 's were measured by following the recovery of the free induction decay following a saturating comb of  $90^\circ$  pulses.

The  $^{183}\text{W}$   $T_1$  results are portrayed graphically in Fig. 2. Figure 3 presents the  $^{183}\text{W}$  Knight-shift results. The zero of Knight shift used in the values for  $K$  was the position of the  $^{183}\text{W}$  resonance in noncubic  $\text{WO}_3$ . The shift between the  $^{183}\text{W}$  res-

onance in tungsten metal and  $\text{WO}_3$  was measured in earlier work<sup>15</sup> as  $+1.062\%$  at 298 K with a variation of no more than  $0.01\%$  down to 4.2 K.<sup>22</sup> Representative absorption line shapes are shown in Fig. 4 with the full widths at half maxima plotted in Fig. 5. The  $^7\text{Li}$  results are listed in Table II.

An attempt was made to observe the  $^{17}\text{O}$  resonance in  $\text{Na}_{0.84}\text{WO}_3$ .  $^{17}\text{O}$  is the only magnetic isotope of oxygen. It has a nuclear moment sixteen times as large as that of  $^{183}\text{W}$  but has a natural abundance of only  $(3.7 \times 10^{-2})\%$ . Nevertheless, calculations indicated that in a bronze sample, the  $^{17}\text{O}$  signal at 14 MHz should be slightly stronger than  $^{183}\text{W}$  at 7 MHz. The attempt at observing the  $^{17}\text{O}$  echo failed. It is possible that the  $^{17}\text{O}$ -conduction-electron coupling is so weak in the bronzes that  $T_1$  is very long, making the iterative signal-averaging process ineffective. Alternatively, or concurrently, the electric quadrupole broadening of the resonance due to a deviation from cubic symmetry at oxygen sites may make the reson-

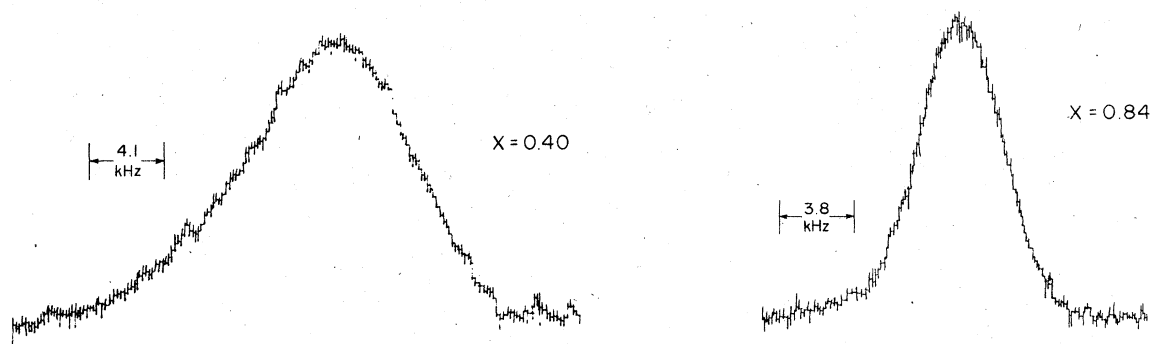


FIG. 4. Representative  $^{183}\text{W}$  absorption line shapes,  $\chi''(\omega)$ , from this work. Direction of increasing frequency is left to right.

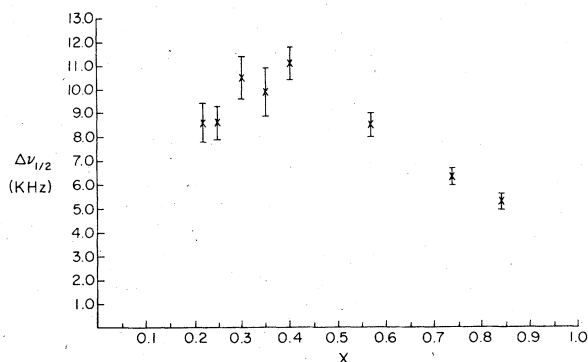


FIG. 5.  $^{183}\text{W}$  linewidths in  $\text{Na}_x\text{WO}_3$ . Full widths at half maxima obtained from absorption line shapes.

ance unobservably broad. Such distortions have been observed in optical birefringence<sup>23</sup> and neutron diffraction<sup>24</sup> studies of the sodium bronzes.

#### INTERPRETATION OF RESULTS

The principal features of the  $^{183}\text{W}$   $K$  and  $T_1$  data in  $\text{Na}_x\text{WO}_3$  may be summarized as follows. Throughout the range of alkali concentrations studied,  $T_1T$  was independent of temperature between 1.35 and 4.2 K indicating the dominance of metallic conduction-electron hyperfine coupling in determining the resonance properties. Consistent with previous results, all the measured  $^{183}\text{W}$  Knight shifts were diamagnetic suggesting that  $5d$  core polarization is the principal coupling mechanism. Over the high alkali concentration range ( $x > 0.40$ ), the  $x$  variations of  $K$  and  $(T_1T)^{-1/2}$  are consistent with the linearly varying Fermi-surface density of states of the  $\text{ReO}_3$ -like  $\text{W } 5d(t_{2g})$  conduction-band model. The range of samples with  $x \geq 0.57$  duplicates the range of  $^{183}\text{W}$  measurements made by Fromhold and Narath.<sup>16</sup> Their results show relaxation rates approximately 30% slower and Knight shifts about 0.03% more negative than those measured in the present work. However, the  $x$  dependence of the data is comparable. In the concentration range  $0.22 \lesssim x \lesssim 0.40$ , both  $K$  and

$(T_1T)^{-1/2}$  deviate from the predictions of linear extrapolation of the high- $x$  results, with the  $K$  data dropping off more sharply than  $(T_1T)^{-1/2}$ . It should be noted that  $x=0.40$  is that concentration at which a sharp change in slope of the  $^{23}\text{Na}$   $(T_1T)^{-1/2}$  data occurs (Fig. 1).

Tunstall<sup>7</sup> has suggested that the enhanced low- $x$   $^{23}\text{Na}$  relaxation rates could result from an increase in the correlation time  $\tau$  of the electronic hyperfine field at the nucleus due to strong scattering of the conduction electrons in the low mobility bronzes. This mechanism was described by Warren<sup>25</sup> in connection with the liquid semiconductors. In the strong scattering situation, in which the mean free path is on the order of the lattice constant, the standard expression for the spin-lattice relaxation rate [Eq. (5)] may no longer be applicable. The derivation of this expression assumed, through suitable averaging over the conduction-electron system with the Fermi function, that a nucleus, in effect, interacts with the entire sea of electrons. In the strong scattering situation,  $T_1^{-1} \propto \tau$  (assuming the nuclear Larmor period is much longer than  $\tau$ ). Thus, as the electron mobility decreases and  $\tau$  increases, an enhancement of the relaxation rate would occur. The electron spends more time around a given nucleus, slowing the fluctuations in the hyperfine field, increasing the correlation time. Warren defined an enhancement parameter  $\eta$  such that:

$$\eta = (T_1)^{-1} / (T_1)_{\text{Korr}}^{-1}, \quad (7)$$

where  $(T_1)_{\text{Korr}}^{-1}$  is the spin-lattice relaxation rate predicted by the Korringa relation (5). Warren further related this parameter to the conductivity.

$$\eta\sigma = \sigma_0. \quad (8)$$

$\sigma_0$  has a typical value of  $3000 (\Omega \text{ cm})^{-1}$ . Thus,  $\eta \approx 3$  at  $x=0.25$ . It is difficult, therefore, to attribute the enhancement in  $T_1^{-1}$  of  $^{23}\text{Na}$  more than partially to this mechanism, since the enhancement experimentally for  $\text{Na}_{0.25}\text{WO}_3$  is greater than 50. Furthermore, such a mechanism would not discriminate between  $^{23}\text{Na}$  and  $^{183}\text{W}$  nuclei, so that equal enhancement of the  $^{183}\text{W}$  and  $^{23}\text{Na}$  rates would be expected. This is inconsistent with the experimental results shown in Figs. 1 and 2.

The persistence of the linear variation of the Fermi-surface density of states, as indicated by the specific-heat and magnetic susceptibility results, coupled with the enhanced  $^{23}\text{Na}$  spin-lattice relaxation rates and the diminished  $^{183}\text{W}$  relaxation rates and Knight shifts suggest there is an alteration in the hyperfine coupling of the conduction electrons to the sodium and tungsten nuclei at concentrations below  $x=0.40$ . These results imply a change in the nature of the conduction-electron wave function

TABLE II.  $^7\text{Li}$  NMR results.

$x$	$T$ (°K)	$K$ (ppm)	$T_1$ (S)
0.27	77	$-8 \pm 8$	$53 \pm 4$
	300		$70 \pm 8$
0.32	77	$9 \pm 13$	$54 \pm 6$
	300		$65 \pm 12$
0.42	77	$-14 \pm 18$	$70 \pm 6$
	300		$35 \pm 6$
0.49	77	$-8 \pm 3$	$70 \pm 6$
	300		$39 \pm 7$

at the Fermi surface.

The expressions for a particular component of the Knight shift and spin-lattice relaxation rate may be written:

$$K_i = \beta^{-1} H_{\text{hf}}^i \chi \alpha_i, \quad (9)$$

$$(T_1)_i^{-1} = 4\pi\hbar(\gamma_n H_{\text{hf}}^i)^2 [\alpha_i \rho(E_F)]^2 kT \delta_i, \quad (10)$$

$$(T_1)^{-1} = \sum_i (T_1)_i^{-1} \text{ and } K = \sum_i K_i. \quad (11)$$

$\rho(E_F)$  is the Fermi surface density of states for one spin direction per unit cell.  $\alpha_i$  is the fractional admixture of a particular wave function.  $H_{\text{hf}}^i$  is the hyperfine field per electron for the  $i$ th component and  $\delta_i$  is the numerical constant for the particular coupling mechanism involved as originally defined in Eq. (5).

Mixing of Na 3s states in the conduction electron wave function is a possible source of the enhanced  $^{23}\text{Na}$  relaxation. S electrons couple to the nucleus through the Fermi contact interaction.

$$H_{\text{hf}}(\text{contact}) = \frac{8}{3} \pi \beta \langle |\Psi(0)|^2 \rangle_{E_F}. \quad (12)$$

$\langle |\Psi(0)|^2 \rangle_{E_F}$  is the wave-function amplitude at the nucleus averaged over the Fermi surface. The susceptibility  $\chi$ , is the spin susceptibility.

$$\chi = \frac{1}{2} (\gamma_e \hbar)^2 \rho(E_F). \quad (13)$$

The magnitude of the sodium 3s component of the conduction-electron wave function in  $\text{Na}_{0.25}\text{WO}_3$  required to produce the observed  $^{23}\text{Na}$  relaxation rate may be determined as follows. For  $\text{Na}_{0.25}\text{WO}_3$ ,  $(T_1)^{-1} = 5 \times 10^{-3} \text{ s}^{-1}$ . From specific-heat data  $\rho(E_F) = 1.3 \times 10^{11} \text{ cgs units per unit cell}$ . The hyperfine field may be estimated from the value of the hyperfine coupling constant for atomic sodium.

$$H_{\text{hf}} = 0.7\pi a(s)c/\gamma_n \quad (14)$$

$a(s) = 0.0296 \text{ cm}^{-1}$  (Ref. 26). The factor 0.7 accounts for the effects of conduction-electron screening. Equation (14) results in a contact hyperfine field for sodium of  $2.8 \times 10^5 \text{ G per Na 3s electron}$ . For the contact interaction  $\delta_i = 1$ . Equation (10) then yields  $\alpha_i = 0.10$ . Thus a 10% sodium 3s character to the conduction-electron wave function at the Fermi surface is sufficient to produce the observed  $^{23}\text{Na}$  spin-lattice relaxation rate in  $\text{Na}_{0.25}\text{WO}_3$ . The Knight shift associated with this interaction may be calculated from (9).  $K_i = +70 \text{ ppm}$ . The  $x$ -independent experimental Knight shift is  $-65 \text{ ppm at 4.2 K}$ , seemingly inconsistent with the theoretical result.

Sodium 3p wave-function admixture is also a possible source of  $^{23}\text{Na}$  low  $x$  relaxation. P electrons, having zero amplitude at the nucleus, will couple only indirectly via the contact term to the nucleus through the core polarization mechanism.

$$H_{\text{hf}}(\text{core polarization}) = \frac{8}{3} \pi \beta |\Psi_{\text{cp}}(0)|^2. \quad (15)$$

$|\Psi_{\text{cp}}(0)|^2$  is the total probability density at the nucleus obtained by summing over all pairs of inner-shell s electrons whose exact spin cancellation is altered by the exchange interaction with the 3p electron. Unrestricted Hartree-Fock calculations<sup>27</sup> indicate that the polarization of the 1s shell is opposite in sign and partially cancels that of the 2s shell of sodium. These calculations yield  $|\Psi_{\text{cp}}(0)|^2 = 3.0 \times 10^{22} \text{ cm}^{-3}$ . Thus for sodium 3p core polarization, the hyperfine field per 3p conduction electron is  $2.4 \times 10^3 \text{ G}$ . For 100% Na 3p character,  $\alpha_i = 1$ , Eq. (10) yields a Knight shift of only 6 ppm, which would constitute only a minor contribution to the observed  $^{23}\text{Na}$  Knight shift. For d electrons,  $\delta$  for core polarization is the reciprocal of the orbital degeneracy.<sup>17</sup> Applying this rule to three degenerate p orbitals,  $\delta_i = \frac{1}{3}$ . This results in a core polarization relaxation rate for  $^{23}\text{Na}$  of  $1.2 \times 10^{-5} \text{ s}^{-1}$  at 4.2 K which is very small compared to the measured rate of  $5 \times 10^{-3} \text{ s}^{-1}$  for  $\text{Na}_{0.25}\text{WO}_3$ . These rough calculations indicate that core polarization would not produce the enhanced sodium relaxation rate even if the entire Fermi-surface conduction-electron wave function were of Na 3p character.

The direct coupling of the orbital and spin dipolar magnetic moments of the 3p electron to the nucleus provide alternate relaxation mechanisms. The coupling of both these moments to the nucleus can provide relaxation mechanisms while having minimal effect on the Knight shift, an effect observed in the  $^{23}\text{Na}$  results. This differentiation is possible because the Knight shift depends upon the average hyperfine field while the spin-lattice relaxation results from the fluctuations. The average spin dipolar interaction is zero in a cubic environment.<sup>28</sup> The orbital 3p Knight shift would likely be small due to quenching of the average orbital magnetic moment. The degree of Na 3p admixture required to produce the observed  $\text{Na}_{0.25}\text{WO}_3$   $^{23}\text{Na}$  relaxation rate via the orbital and spin dipolar interactions may be estimated as well.

$$H_{\text{hf}}(\text{orbital spin}) = 0.7(2\beta)\langle r^{-3} \rangle. \quad (16)$$

$\langle r^{-3} \rangle$  is an expectation value for the Na 3p orbital. For the orbital mechanism  $\delta_i = \frac{2}{9}$ , for the spin dipolar  $\delta_i = \frac{1}{15}$ , for p electrons.<sup>29</sup> Thus, the total relaxation rate from these two mechanisms is:

$$(T_1)^{-1} = \frac{13}{45} 4\pi\hbar[\gamma_n(2\beta)(0.7)\langle r^{-3} \rangle]^2 \alpha_i^2 \rho(E_F) kT. \quad (17)$$

From atomic beam measurements<sup>30</sup>  $\langle r^{-3} \rangle = 1.7 \times 10^{24} \text{ cm}^{-3}$  for sodium 3p state, which results in a hyperfine field of  $2.2 \times 10^4 \text{ G}$ . From Eq. (17), then,

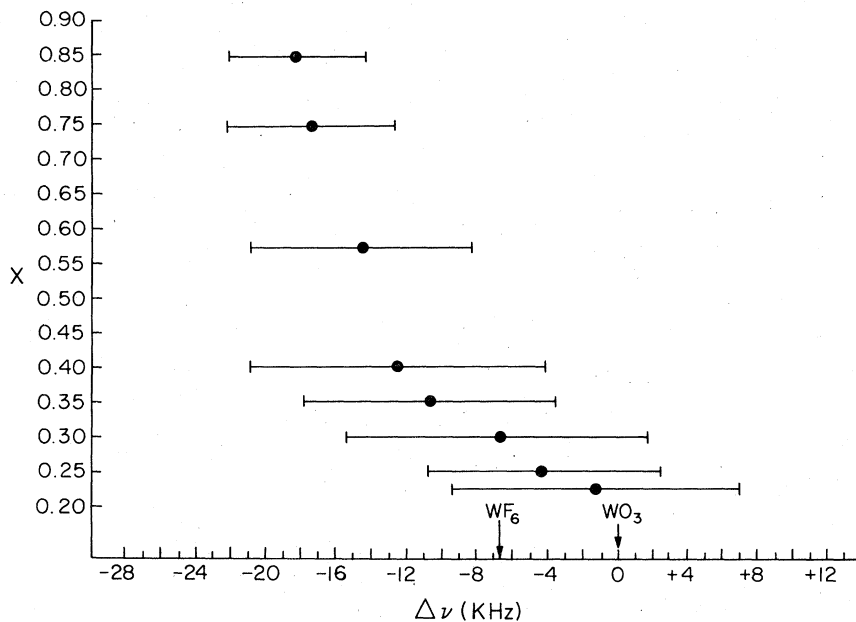


FIG. 6. Spread and position of  $^{183}\text{W}$  resonances in  $\text{Na}_x\text{WO}_3$  (full widths at  $\frac{1}{5}$  maxima).

$\alpha_i = 2.3$ . Since  $\alpha_i = 1$  would imply 100% Na 3p character to the wave function, this result indicates that the orbital and spin dipolar hyperfine coupling of 3p conduction electrons as described by Eqs. (10) and (17) would be inadequate to account for the observed  $^{23}\text{Na}$   $\text{Na}_{0.25}\text{WO}_3$  relaxation rate. To make this model tractable, an enhanced relaxation, perhaps due to strong scattering, with  $\eta$  at least 5, must be invoked.

The models presented based on a partial shift in the nature of the conduction-electron wave function at low  $x$  from W 5d to Na 3s or 3p are in rough qualitative agreement with the  $^{183}\text{W}$   $K$  and  $T_1$  data. These models predict a weakening of the electronic coupling to the  $^{183}\text{W}$  nuclei and therefore diminished Knight shifts and relaxation rates. However, alone, these models are unable to account for the more precipitous drop of the Knight-shift data below  $x = 0.40$ . Furthermore, the  $^{183}\text{W}$  Knight shifts coupled with the line-shape results (Fig. 6) indicate that for the lowest- $x$  samples, parts of the absorption lines actually correspond to *positive* Knight shifts. These positive shifts are difficult to explain solely in terms of 5d core polarization. Thus the possibility exists of a partial W 6s admixture. The hyperfine coupling constant for  $^{183}\text{W}$  is  $a(s) = 0.065 \text{ cm}^{-1}$ , so that the contact W 6s hyperfine field would be  $+2.9 \times 10^6 \text{ G}$ . The deviation of the  $^{183}\text{W}$  Knight shift at  $x = 0.25$  from the extrapolated high- $x$  value is about +0.1%. Assuming +0.03% of this deviation is due to a 20% reduction in the 5d character of the wave function, employing Eq. (9) results in  $\alpha_i = 0.08$ . Thus an 8% W 6s component to the conduction-electron wave func-

tion would produce the observed positive deviation in the  $\text{Na}_{0.25}\text{WO}_3$   $^{183}\text{W}$  Knight shift. The accompanying 6s contact spin-lattice relaxation rate at 4.2 K from Eq. (11) would be  $1.5 \times 10^{-2} \text{ s}^{-1}$  and would be a non-negligible contribution to the observed rate of  $9 \times 10^{-2} \text{ s}^{-1}$ . Although the 6s contribution to the Knight shift would be opposite in sign to the 5d core polarization shift, the relaxation rate would provide a small *addition* to the total relaxation rate. Therefore, the low- $x$   $^{183}\text{W}$  Knight shifts would be expected to drop more sharply than the relaxation rates, consistent with experimental results.

The  $x$  dependence of the  $^{183}\text{W}$  Knight shifts in  $\text{Li}_x\text{WO}_3$  is similar to the  $\text{Na}_x\text{WO}_3$  data. In the range  $0.27 \leq x \leq 0.49$ , the slopes of the  $K$  vs  $x$  plots appear similar. Unfortunately,  $\text{Li}_x\text{WO}_3$  crystals with concentrations much greater than 0.40, the turning point on the  $\text{Na}_x\text{WO}_3$  Knight-shift plot, cannot be grown. The  $\text{Li}_{0.49}\text{WO}_3$   $^{183}\text{W}$  Knight shift hints that the slope might be changing. However, within the limits of experimental uncertainty, such an assertion cannot be made with a clear conscience. The  $^{183}\text{W}$   $T_1$ 's and  $T_2$ 's are comparable to their  $\text{Na}_x\text{WO}_3$  counterparts, so that the  $^{183}\text{W}$  results in  $\text{Li}_x\text{WO}_3$  give no clear indication that the  $\text{Li}_x\text{WO}_3$  and  $\text{Na}_x\text{WO}_3$  systems are very different.

There appears a contrast between  $\text{Na}_x\text{WO}_3$  and  $\text{Li}_x\text{WO}_3$  in the NMR properties of the alkali nuclei. For  $\text{Na}_{0.25}\text{WO}_3$ , the  $^{23}\text{Na}$   $T_1$  was measured as 2.1 s at 77 K. This may be compared with the  $^7\text{Li}$  relaxation time at 77 K for  $\text{Li}_{0.27}\text{WO}_3$  of 53 s. For magnetic conduction-electron relaxation via  $s$  electrons  $(T_1)^{-1}$  is proportional to  $[\gamma_n a(s)]^2$ . There-

fore if for  $\text{Li}_{0.27}\text{WO}_3$  the same admixture of Li 2s as Na 3s wave function is assumed, then using values of  $a(s)$  from Knight,<sup>26</sup> the  ${}^7\text{Li}$   $T_1$  should be only 2.3 times as long as the  ${}^{23}\text{Na}$   $T_1$ .

The  ${}^{183}\text{W}$  resonance in  $\text{Na}_x\text{WO}_3$  exhibits an inhomogeneously broadened absorption line. The spread in frequency of the line is much greater than would be predicted by  $T_2$ , the spin-echo phase memory time, which is governed by  ${}^{183}\text{W}$ - ${}^{183}\text{W}$  nuclear-spin coupling.  $T_2$  is about 25 ms for  ${}^{183}\text{W}$  in  $\text{Na}_x\text{WO}_3$ .<sup>16</sup> Thus the width of the  ${}^{183}\text{W}$  resonance if determined by the distribution of local fields due to the dipolar fields from neighboring nuclei would only be about 20 Hz. The width of the magnet inhomogeneity field distribution was less than 1 kHz across the sample. Whereas, the experimental linewidths ranged from 5 to 11 kHz. Clearly, the  ${}^{183}\text{W}$  lines are broadened by a distribution of local environments logically related to the random occupancy of sodium sites. As the  ${}^{183}\text{W}$  nucleus has a zero-electric-quadrupole moment, a distribution of local Knight shifts is the most likely source of the broadening. The linewidths are appreciable compared to the total range of  ${}^{183}\text{W}$  Knight shifts in  $\text{Na}_x\text{WO}_3$  indicating a wide range of local  ${}^{183}\text{W}$  environments in each sample. For a random distribution of filled alkali sites, Gaussian absorption line shapes would be expected, assuming  $H_{\text{hf}}$  is independent of  $x_{\text{local}}$ . Further, since in such a random-distribution model 50% occupancy provides the greatest number of equivalent arrangements, a linewidth dependence upon  $x$  which is peaked at  $x=0.50$  would be expected. The line shapes for the two highest  $x$  samples exhibit a definite Gaussian shape (the  $x=0.84$  line is shown in Fig. 4). However, a clear asymmetry develops in the lines for  $x \leq 0.57$  (note the  $x=0.40$  line also shown in Fig. 4). This asymmetrical broadening is also evidenced in Fig. 5 which shows the low- $x$  linewidths not dropping off as would be expected from a simple random distribution model. These results are not surprising, as the  $K$  and  $T_1$  results indicate that  $H_{\text{hf}}$  is  $x$  dependent below  $x=0.40$ . It is also logical that the slight asymmetry first appears in the  $x=0.57$  line. In the  $\text{Na}_{0.57}\text{WO}_3$  lattice, substantial regions undoubtedly exist for which  $x_{\text{local}} < 0.40$ .

## CONCLUSIONS

### Band structure

The following model appears to provide the simplest and most consistent explanation of the NMR results. For large alkali concentration ( $x > 0.40$ ), the cubic  $\text{Na}_x\text{WO}_3$  band structure is adequately described in terms of a rigid  $\text{ReO}_3$ -like W  $5d(t_{2g})$  conduction band with the alkali atom donating its

valence electron to this band, and the Fermi surface density of states varying linearly with  $x$ .

Below  $x=0.40$  the enhanced  ${}^{23}\text{Na}$  relaxation rates and the diminished  ${}^{183}\text{W}$  Knight shifts and relaxation rates suggest an alteration in the nature of the Fermi-surface conduction-electron wave function. Admixture of Na  $3p$  states in the low- $x$  wave function inadequately accounts for the enhanced  ${}^{23}\text{Na}$  relaxation as the Na  $3p$  hyperfine coupling is too weak. A model requiring at  $x=0.25$  only 10% Na 3s along with 8% W 6s character to the wave function is more consistent with a variety of experimental results. The conduction band in this model retains the essential W  $5d$  character at low  $x$  and consequently the Fermi-surface density of states which varies linearly with  $x$ . The sodium component of the wave function provides a mechanism for the enhanced  ${}^{23}\text{Na}$  low- $x$  relaxation rates. The decrease in the tungsten character of the wave function at low  $x$  diminishes the  ${}^{183}\text{W}$  relaxation rates while the W 6s component provides a positive contribution to the  ${}^{183}\text{W}$  Knight shift, causing its sharp low- $x$  decline. The reason for the absence of the Na 3s paramagnetic contribution to the Na Knight shift is somewhat unclear. The high- $x$  negative  ${}^{23}\text{Na}$  Knight shifts are attributable to polarization of the  ${}^{23}\text{Na}$  core due to the overlap of W  $5d$  electrons. Perhaps the alteration of this core polarization by the admixture of the spatially more extensive W 6s state could provide an additional negative component to the  ${}^{23}\text{Na}$  shift explaining the apparent discrepancy.

### Metal-semiconductor transition

The variation of the  ${}^{23}\text{Na}$   $T_1$  data with  $x$  indicates the conduction electrons are not confined to metallic clusters with local density  $x=1$  as is proposed in simple percolative conduction models of the bronzes which assume only nearest-neighbor linkages between cells with filled alkali sites.<sup>31,32</sup> If such were the case, the NMR properties of  ${}^{23}\text{Na}$  would be  $x$  independent, since all  ${}^{23}\text{Na}$  nuclei would be contained in metallic clusters looking like  $\text{NaWO}_3$ . Only the size and number of these regions would change with  $x$ . The recent correlated site percolation picture of Webman *et al.*<sup>31</sup> which hypothesized nonrandom clustering of filled alkali sites in metallic clusters of 100 Å extent also appears inconsistent with the  ${}^{183}\text{W}$  absorption line shapes. The broad  ${}^{183}\text{W}$  absorption lines suggest a distribution of local environments incompatible with appreciable nonrandom clustering. Percolation ideas undoubtedly have some validity for alkali concentrations near the metal-semiconductor transition in a disordered system such as the bronzes. However, to extend this picture to con-

centrations much above the transition does not seem warranted. Observation of metallic pockets in semiconducting bronze crystals, would give credence to percolative ideas close to the transition. Unfortunately such efforts have been hampered by the inability to grow cubic samples on the semiconducting side of the transition.

There seems little evidence to support the hypothesis of a Mott-type transition<sup>33</sup> in the bronzes. There is no firm indication, like the enhanced and temperature-dependent magnetic susceptibility and Knight shift in the Si:P system,<sup>34-36</sup> to suggest that close to the transition the conduction electron gas is highly correlated in the bronzes. Throughout the entire range of concentrations studied, the <sup>183</sup>W Knight shifts evidenced no temperature dependence between 1.35 and 4.2 °K.

Mott<sup>37</sup> recently has proposed the occurrence of Anderson localization at  $x=0.20$  in the cubic bronzes. The bronzes certainly qualify as a disordered system in the Anderson sense, and the temperature dependence of the Hall constant and conductivity below  $x=0.25$ <sup>2</sup> do suggest the approach of the Fermi level to a mobility edge. However, the experimental evidence does not warrant a firm acceptance of this model at this time.

#### ACKNOWLEDGMENTS

The guidance of Professor Donald F. Holcomb throughout the course of this work is gratefully acknowledged. Also of great benefit were the contributions of Dr. Gerard A. Tinelli, Dr. David P. Tunstall, and David A. Lilienfeld.

\*This work was supported in part by the National Science Foundation, through Grant No. GH-32250 and through the Cornell Materials Science Center.

†Present address: Physics Department, University of Pennsylvania, Philadelphia, Pa. 19104.

- <sup>1</sup>H. R. Shanks, *J. Crystallogr. Growth* **13-14**, 433 (1972).
- <sup>2</sup>P. A. Lightsey, D. A. Lilienfeld, and D. F. Holcomb, *Phys. Rev. B* **14**, 4730 (1976).
- <sup>3</sup>L. D. Muhlestein and G. C. Danielson, *Phys. Rev.* **158**, 825 (1967).
- <sup>4</sup>W. McNeil and L. E. Conroy, *J. Chem. Phys.* **36**, 87 (1962).
- <sup>5</sup>L. F. Mattheiss, *Phys. Rev. B* **6**, 4718 (1972).
- <sup>6</sup>L. F. Mattheiss, *Phys. Rev.* **181**, 987 (1969).
- <sup>7</sup>D. P. Tunstall, *Phys. Rev. B* **11**, 2821 (1975).
- <sup>8</sup>F. C. Zumsteg, Jr., *Phys. Rev. B* **14**, 1406 (1976).
- <sup>9</sup>R. W. Vest, M. Griffel, and J. F. Smith, *J. Chem. Phys.* **28**, 293 (1958).
- <sup>10</sup>J. D. Greiner, H. R. Shanks, and D. C. Wallace, *J. Chem. Phys.* **36**, 772 (1962).
- <sup>11</sup>F. Kupka and M. J. Sienko, *J. Chem. Phys.* **18**, 1296 (1950).
- <sup>12</sup>W. A. Kamitakahara, B. N. Harmon, J. G. Taylor, L. Kopp, and H. R. Shanks, *Phys. Rev. Lett.* **36**, 1393 (1976).
- <sup>13</sup>W. Jones, E. Garbaty, and R. Barnes, *J. Chem. Phys.* **36**, 494 (1962).
- <sup>14</sup>A. T. Fromhold and A. Narath, *Phys. Rev.* **136**, 487 (1964).
- <sup>15</sup>A. Narath and D. Wallace, *Phys. Rev.* **127**, 724 (1962).
- <sup>16</sup>A. T. Fromhold and A. Narath, *Phys. Rev.* **152**, 585 (1966).
- <sup>17</sup>Y. Yafet and V. Jaccarino, *Phys. Rev.* **133**, 650 (1964).

- <sup>18</sup>P. A. Lightsey, *Phys. Rev. B* **8**, 3586 (1973).
- <sup>19</sup>B. W. Brown and E. J. Banks, *J. Am. Chem. Soc.* **76**, 963 (1954).
- <sup>20</sup>M. Wechter, H. R. Shanks, and A. Voight, *Inorg. Chem.* **7**, 845 (1968).
- <sup>21</sup>W. G. Clark, *Rev. Sci. Instrum.* **35**, 316 (1964).
- <sup>22</sup>A. Narath and A. T. Fromhold, *Phys. Rev.* **139**, 794 (1965).
- <sup>23</sup>J. H. Ingold and R. C. DeVries, *Acta Metall.* **6**, 736 (1958).
- <sup>24</sup>M. Atoji and R. E. Rundle, *J. Chem. Phys.* **32**, 627 (1960).
- <sup>25</sup>W. W. Warren, Jr., *Phys. Rev. B* **3**, 3708 (1971).
- <sup>26</sup>W. D. Knight, *Solid State Physics*, edited by F. Seitz and D. Turnbull (Academic, Oxford, 1956), Vol. II, p. 120.
- <sup>27</sup>D. A. Goodings, *Phys. Rev.* **123**, 1706 (1961).
- <sup>28</sup>N. Bloembergen and T. J. Rowland, *Acta Metall.* **1**, 731 (1953).
- <sup>29</sup>Y. Obata, *J. Phys. Soc. Jpn.* **18**, 1020 (1963).
- <sup>30</sup>M. L. Perl, I. I. Rabi, and B. Senitzky, *Phys. Rev.* **98**, 611 (1955).
- <sup>31</sup>I. Webman, J. Jortner, and M. H. Cohen, *Phys. Rev. B* **13**, 713 (1976).
- <sup>32</sup>R. Fuchs, *J. Chem. Phys.* **42**, 3781 (1965).
- <sup>33</sup>N. F. Mott, *Philos. Mag.* **6**, 287 (1961).
- <sup>34</sup>J. D. Quirt and J. R. Marko, *Phys. Rev. B* **7**, 3842 (1973).
- <sup>35</sup>W. Sasaki, S. Ikehata, and S. Kobayashi, *J. Phys. Soc. Jpn.* **36**, 1377 (1974).
- <sup>36</sup>G. C. Brown and D. F. Holcomb, *Phys. Rev. B* **10**, 3394 (1974).
- <sup>37</sup>N. F. Mott, *Philos. Mag.* **35**, 111 (1977).